Gain and Noise in THz MgB_2 Hot-Electron Bolometer Mixers With a 30-K Critical Temperature

Evgenii Novoselov and Sergey Cherednichenko

***Abstract*—In this paper, we study variation of the MgB_2 hot-electron bolometer mixer characteristics such as noise temperature, gain, output noise, and local oscillator (LO) power at 5-, 15-, and 20-K bath temperatures, and at 0.69- and 1.63-THz LO frequencies. The main reason for the noise temperature rising at higher temperatures is a reduction of the mixer gain, which occurs proportionally to the LO power reduction. Contrary to this, the output noise remains constant (for the same bias point).**

***Index Terms*—Hot-electron bolometer (HEB), hybrid physical chemical vapor deposition (HPCVD), magnesium diboride, mixer, superconductivity, thin film.**

I. Introduction

SUPERCONDUCTING hot-electron bolometer (HEB) mixers made from thin MgB_2 films have demonstrated a noise temperature of $\sim$1000 K and a noise bandwidth (NBW) of 11 GHz at local oscillator (LO) frequencies of 0.69 and 1.63 THz [1]. When comparing previously published results [2]–[7], this progress was made owing to advances in thin MgB_2 films deposition by hybrid physical chemical vapor deposition (HPCVD), where films thinner than 10 nm with a critical temperature (T_c) above 30 K have been obtained [8]–[11]. When the mixer operation temperature was raised from 5 to 15 K only a small increase of the receiver noise temperature, T_r has been observed (20%). However, when the mixer temperature was increased to 20 K, the noise temperature rose by another 50%. The origin of this effect is of great importance to future HEB performance improvement. In this paper, we study how the major HEB mixer characteristics, such as the noise temperature, the gain, the output noise, and the LO power, vary through an operation temperature range of 5–20 K. The mixer parameters most critical to mixer low noise operation up to 20 K (or above) are discussed.

II. Devices and Setup

In this study, mixers from the same batch as reported in [1] were used. In brief, MgB_2 films were deposited on SiC substrates using HPCVD [11]. The HEB mixers were essentially 1 μm $\times$ 1 μm microbridges integrated with a 270-nm-thick gold planar spiral antenna [3]. The MgB_2 film thickness was measured on one of the devices from this batch using transmission electron microscopy. The measured film thickness of 8 nm was slightly higher than the value (6 nm) estimated from the deposition rate (obtained for thicker films). The critical temperature in the devices after patterning and dicing was 30 K (see Fig. 1).

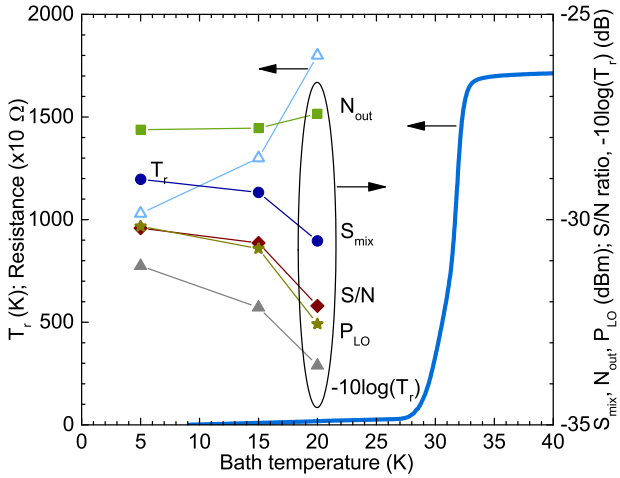

Fig. 1. Mixer output noise $N_{\mathrm{out}}\mathrm{dB}$ (squares, 50-MHz bandwidth), the mixing signal $S_{\mathrm{mix}}\mathrm{dB}$ (circles), *signal-to-noise* ratio *S/N* dB (diamonds) (shifted by $+73$, $+57$, and -45 dB, respectively), T_r (open triangles), $-10\log(T_r)$ (triangles), and LO power (P_{LO}) (shifted by $+10$ B), versus temperature. Normalization factors were applied for fitting all curves on the single figure. Resistance ($\times 10$) versus temperature (solid line). Mixer characteristics were measured at 7 mV and 0.23 mA bias for all temperatures. LO frequency is 0.69 THz.

The HEBs were tested in a quasi-optical mixer block with an uncoated 5-mm-elliptical Si lens. A 30-mm-diameter off-axis aluminum parabolic mirror collimated the THz beam prior to exit from the cryostat. A bias-T and a low-noise IF amplifier (LNA) were mounted in the cryostat. The mixer temperature was varied by means of a resistive heater mounted onto the mixer block. A far infrared gas laser was used as the LO. Previously, we have reported [1] that LO pumped current voltage (IV) curves of the discussed devices were the same for LO frequencies of 0.69, 1.63, and 2.56 THz. As the LO frequency increases from 0.69 to 1.63 THz, rather small growth of the receiver noise temperature (from 830 to 930 K) was observed. Therefore, experiments reported here were performed at 0.69-THz LO, due to a higher output power being available as compared to, e.g., 1.63 THz, as well as due to the availability of another 0.69 THz tunable source used for the mixing experiments. The receiver noise temperature was measured with the Y-factor technique,

Manuscript received September 22, 2017; accepted October 2, 2017. Date of publication October 23, 2017; date of current version November 8, 2017. This work was supported by the European Research Council under the Starting Grant TERAMIX. *(Corresponding Author: Sergey Cherednichenko.)*

The authors are with the Department of Microtechnology and Nanoscience, Chalmers University of Technology, Göteborg SE-41296, Sweden (e-mail: evgenii@chalmers.se; serguei@chalmers.se).

Color versions of one or more of the figures in this paper are available online at http://ieeexplore.ieee.org.

Digital Object Identifier 10.1109/TTHZ.2017.2760105

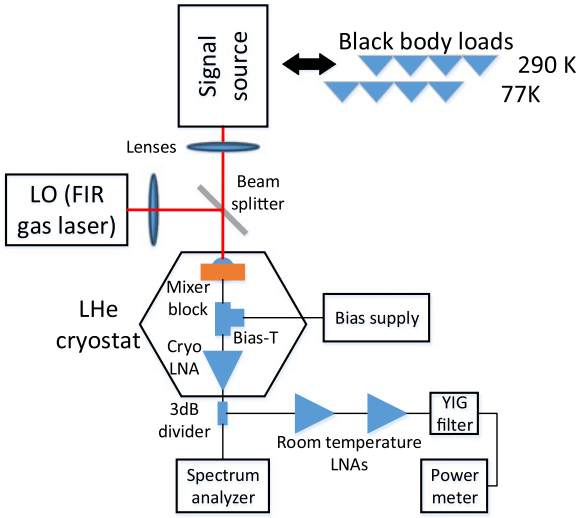

Fig. 2. Measurement setup.

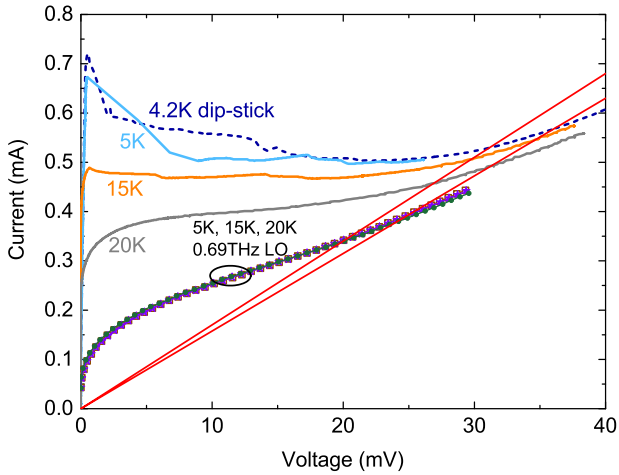

Fig. 3. Mixer IV-curves: at 4.2 K (in the dip-stick, dashed); in the cryostat (≈5 K, no LO, blue), at 15 K (no LO, orange), at 20 K (no LO, grey). Three (fully overlapping) IVs at optimal LO power at 5, 15, and 20 K (open squares, stars, and circles). Straight lines are used for LO power calculations by the isothermal method.

using a 295-K and a 77-K black body emitter (loads). The variation of the mixer (relative) gain was measured with a monochromatic THz signal source, based on frequency multipliers (see Fig. 2) [12]. The absolute power of the signal source (including mixer-to-source beam mismatch losses) was of no importance at that stage. However, the output power of the signal source was kept constant during all experiments. Based on the measured mixer gain (see Section III-b), we estimate an incident power of 10 pW. The IF signal was split into two branches outside the cryostat: 1) with an extra LNA and a tunable bandpass YIG filter (for the Y-factor and the output noise measurements); and 2) directly fed into a spectrum analyzer. The YIG-filter was set at a 2 GHz ($B_{\rm if} = 50$ MHz bandwidth). Both the output noise power and the mixing signal power were corrected for the gains of the corresponding amplifier chains, hence being referenced both to the output of the HEB mixer.

The test source frequency was 695.5 GHz, i.e., 2.5 GHz off-set from the LO, in order to exclude any effect from the test source on the reading from the black body source. For consistency, we accounted for losses in the optical path (the humid air absorption, the cryostat window, and the IR filter) in the receiver noise temperature measurements. Details on optical loss correction are given in [1]. Neither the Si lens reflection loss nor the beam splitter reflection loss is accounted for. The results for the two tested devices (#10–7 and #10–8) from the discussed batch were very similar. Therefore, we concentrated on results from device #10–7 without loss of generality.

The HEB critical current was 0.67 mA at 5 K, corresponding to a critical current density of 8.4×10^6 A/cm^2. At both 5 and 15 K, the IV had a distinct critical current (switch-type IV), whereas at 20 K a smooth flux-flow type of IV has been observed (see Fig. 3). The aforementioned critical current density is of the same order of magnitude as reported before for films of the same thicknesses ($\leq$10 nm) but obtained using a thinning-down technique [9], [10]. Room temperature and residual resistances of the discussed device are 196 and 170 Ω, respectively.

III. Results

A. Bias Optimization

Receiver noise temperature was measured using the Y-factor technique at various LO power levels and in a bias voltage range up to 25 mV. The corresponding set of IVs (each relates to a certain LO power) is given in Figs. 4(a)–6(a) for mixer temperatures 5, 15, and 20 K. The receiver noise temperature measured along IV-5 (at 5 and 15 K) is given in Figs. 4(a) and 5(a) (filled dark cyan squares, right *Y*-axis). In Fig. 4(a), for a bias voltage of 7 mV, T_r as a function of mixer current (hence, LO power) is shown in purple balls (top *X*-axis). The lowest noise temperature is obtained for voltages corresponding to the maximum output noise, i.e., 5–10 mV. The IV-range for the lowest T_r is marked with the red-oval. At 5 K, a constant T_r is obtained at a variety of LO powers corresponding to IV-3–IV-5. As the mixer temperature increases, the optimal LO power range decreases. At 20 K, the lowest T_r can be achieved at around IV-5 only. The lowest receiver noise temperatures obtained at 5, 15, and 20 K are plotted in Fig. 1 (open triangles). They correspond to IV-5 (7 mV, 200 μA).

With the second THz source, detuned by 2.5 GHz from the LO, the mixing signal $P_{\rm if}$ was recorded for the same IVs along with the receiver output noise power $P_{\rm out}$

$$P_{\rm if} = P_S \cdot \frac{1}{L_{\rm opt}} \cdot G_m \cdot G_{\rm if} \tag{1}$$

$$P_{\rm out} = \left(T_{\rm out} + 2 \cdot 300\ {\rm K} \cdot \frac{1}{L_{\rm opt}} \cdot G_m + T_{\rm if}\right) G_{\rm if} \cdot K_B \cdot B_{\rm if} \tag{2}$$

where $L_{\rm opt}$ is the optical loss, $G_{\rm if}$ and $T_{\rm if}$ are the IF chain gain and the noise, respectively, $B_{\rm if}$ is the YIG-filter bandwidth, k_B is the Boltzmann constant, and $T_{\rm out}$ is the HEB mixer output noise. Correcting for the IF chain gain, $G_{\rm if}$, we plot the mixer output signal $S_{\rm mix} = P_{\rm if}/G_{\rm if}$ in Figs. 4(c)–6(c).

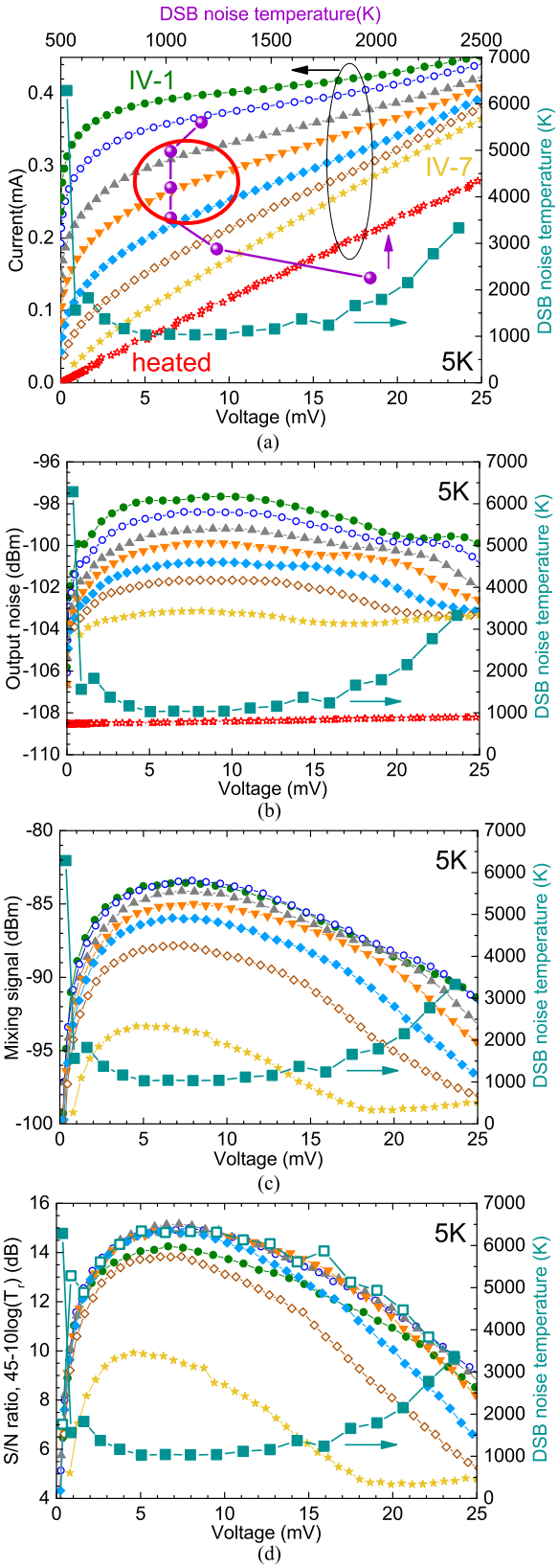

Fig. 4. LO at 0.69 THz. $T = 5$ K. The area of the highest S/N ratio is marked on the IV plane. The open squares in (d) are for $45 - 10\log(T_r)$.

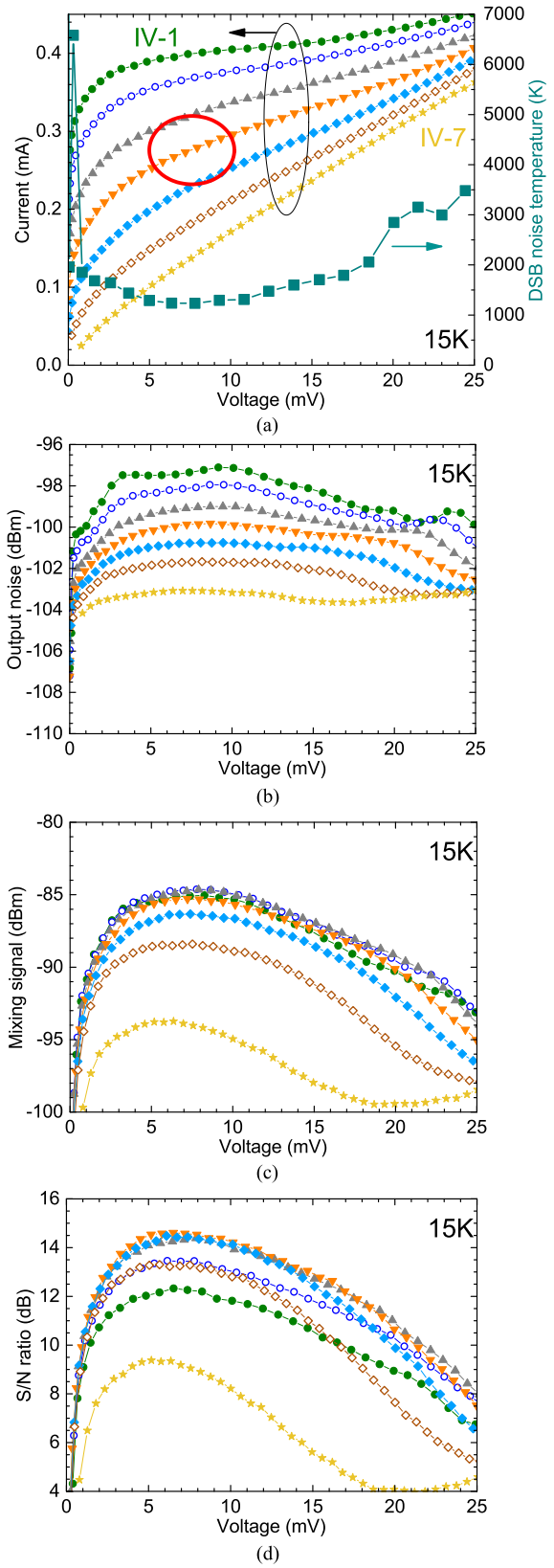

Fig. 5. LO at 0.69 THz. $T = 15$ K. The area of the highest S/N ratio is marked on the IV plane.

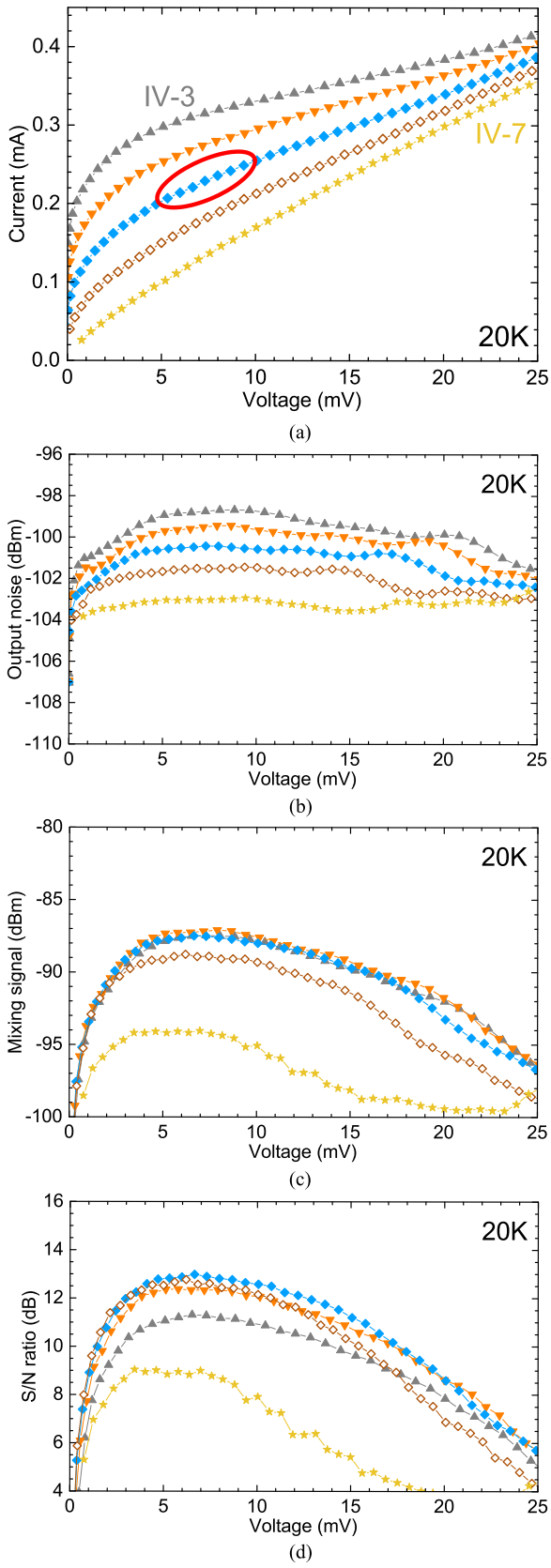

Fig. 6. LO at 0.69 THz. $T = 20$ K. The area of the highest S/N ratio is marked on the IV-plane.

Since the incident THz signal power P_s was constant through the whole experiment, variations of the IF signal $S_{\rm mix}$ are due to changes of the mixer gain G_m, as shown in (1). Therefore, the mixer gain (in relative units) can be compared at different LO power levels and mixer temperatures [see Figs. 4(c)–6(c)].

In order to calculate the HEB output noise $T_{\rm out}$ from (2), we utilized the HEB conversion gain G_m at the optimal point as described in Section III-B. Variations of G_m away from the optimal point were obtained from variation of $S_{\rm mix}$. The corrected output noise, namely $N_{\rm out} = T_{\rm out} \times k_B \times 50$ MHz, is plotted in Figs. 4(b)–6(b). Therefore, during this experiment we measure both variations of mixer gain and output noise, simultaneously.

For the given set of IVs, which more than covers the optimal LO-bias voltage range, the mixer output noise [see Figs. 4(b)–6(b)] increases continuously as the LO power is reduced from IV-7 (overpumped HEB) to IV-1 (underpumped HEB). The mixer gain starts to saturate just above IV-3, hence above the optimal bias zone. The resulting signal-to-noise ratio (S/N) [see Figs. 4(d)–6(d)] has a maximum at IVs-3-5. The (A-log($T_{\rm r}$)) for IV-5 is also plotted in Fig. 4(d), where $A = 45$ dB is a free coefficient used to place this curve close to the measured *S/N* curve. The log-function of $T_r(V)^{-1}$ closely follows the *S/N*(V) curve, as is expected for the ideal case

$$\log(S/N) = \log\left(\frac{P_S}{T_r \cdot B_{if} \cdot k}\right) \propto -\log(T_r) \qquad (3)$$

where k is the Boltzmann constant. Comparing Fig. 4(a) and (d), we conclude that bias voltage–LO power optimizations for both *S/N* and T_r coincide across the IV-plane. This fact demonstrates that, despite the broadband antenna used with the mixer, the "direct detection" effect has no impact on the choice of mixer operation point. The discussed "direct detection" effect is a shift in the HEB bias point when the receiver input load switches from 300 to 77 K. In a 3-THz band, a black body at 300 K (77 K) emits approximately 2.8 nW (1.6 nW) in the single spatial mode [13]. This is about 1% of the optimal LO power for NbN HEB mixers, and hence a switch of the load temperature changes the mixer bias point. For NbN HEB mixers, this effect can be detrimental, either decreasing or increasing the Y-factor, and hence the apparent receiver noise temperature. The effect has been reported to be more pronounced at smaller bias voltages. Our results show that for discussed MgB_2 HEB mixers, although integrated with a broadband antenna, the direct detection effect is negligible.

Furthermore, measurements of the *S/N* ratio allow us for a much larger dynamic range compared to the Y-factor. Instabilities of the LO source sometimes lead to receiver output power fluctuations as large as 0.1 dB. This fact limits applicability of the Y-factor technique to mixer operation points (IV-plane) corresponding to the highest sensitivity (highest Y-factor). To verify the validity of physical models, experimental data well off the sensitive points would be required. Furthermore, the Y-factor technique can be applied mostly to mixers already having quite good sensitivity, e.g., $T_r < 10000$ K ($Y > 0.1$ dB).

B. Mixer Characteristics Versus Temperature

Two types of analyses can be performed in order to compare HEB mixer operation at different temperatures. First, the form of all corresponding IV, $N_{\rm out} - V$, and $S_{\rm mix} - V$ curves at 5, 15, and 20 K is the same (see Figs. 4–6). In order to perform a more precise comparison, we plotted three sets of the curves (corresponding to IVs 3–5) on the same figure (see Fig. 7). For a certain temperature, we find an IV totally matching an IV at another temperature by changing the LO power [see Fig. 7(a)] (see [1]). For the matching IVs, $N_{\rm out} - V$ curves also closely overlap each other. This may only be possible if the mixer output noise temperature, $T_{\rm out}$, is independent of mixer temperature (for the matching IVs). In Fig. 1, $N_{\rm ou}$ (in dBm) is plotted as a function of mixer temperature (all for 7 mV and 200 μA [IV-5, lowest T_r point)].

The absorbed LO was calculated using a constant resistance line, intersecting both the LO pumped and unpumped IVs (the isothermal method [14]). The isothermal method is based on an assumption that both the dc current and the THz LO have the same effect on the HEB dc resistance. This can only be true for HEBs close to the normal state both with and without LO pumping. The utilized constant resistance lines are shown in Fig. 3. For those, the calculated LO power at 5 K is 10.6 and 9.6 μW. Another approach, such as recording two IVs with close LO power levels with a known attenuation, also gives a value close to 10 μW. Moreover, we verified that the LO power variation induced by a wire grid attenuator corresponds to the variation of the LO power calculated from the constant resistance line. A similar observation was made for LO power variations versus temperature. $P_{\rm LO}$ (in dBm) is plotted in Fig. 1 (stars) along with the mixer relative gain, $S_{\rm mix}$ (in dBm) (circles).

In contrast to $N_{\rm out}$, mixer gain decreases at higher temperatures [see Figs. 7(c) and (1)]. It can be observed that when the bath temperature increases from 5 to 20 K, reduction of mixer gain (by 2.5 dB) is proportional to reduction of LO power (by 2.4 dB) for the given IV, as, in fact, would be expected considering the classical HEB mixer model [15].

$-10\log(\rm T_r)$ (where T_r was measured using the Y-factor approach) follows exactly the same temperature trend as the *S/N* ratio, measured using the mixing approach (Fig. 1, filled triangles and diamonds).

Mixer conversion gain (filled circles) and output noise temperature (filled squares), calculated using the U-factor technique with the HEB in the normal state as in [3], are plotted in Fig. 8 for 5-, 15-, and 20-K bath temperatures (all at the same bias point of 7 mV and 0.23 mA). Mixer gain is inversely proportional to the temperature, whereas output noise remains almost the same. This is also confirmed by the mixing experiment, as can be seen in Fig. 1.

As follows from Figs. 4 and 5 (corresponding to mixer temperatures of 5 and 15 K), receiver noise temperature is constant over quite a wide range of LO power levels. Across this range (IV5–IV3), both mixer gain and output noise vary by a factor of 2: from 120 to 220 K and from -10.7 to -8.3 dB, respectively

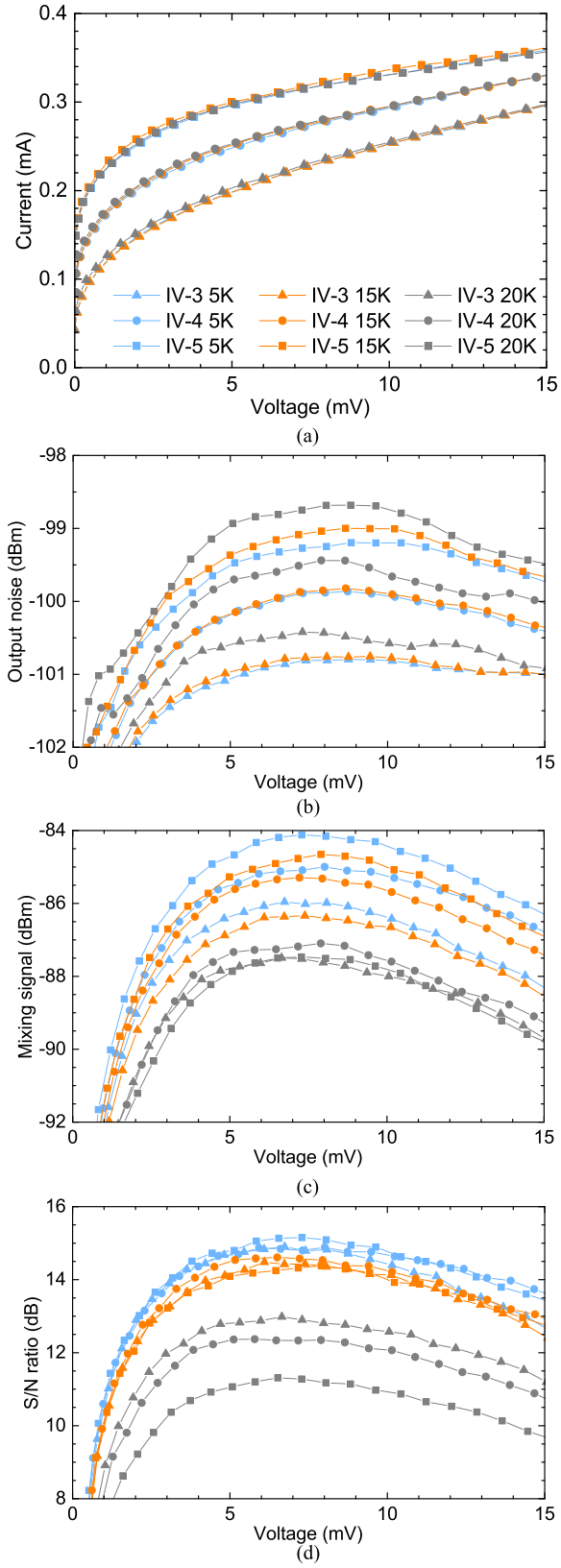

Fig. 7. LO at 0.69 THz. $T = 5$, 15, and 20 K. Close comparison of the IV, P-V, G-V, and S/N-V at the bias voltages and LO power levels corresponding to the highest S/N ratio.

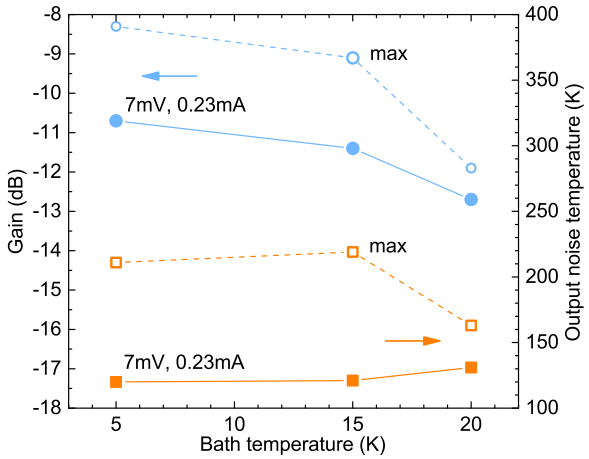

Fig. 8. Mixer gain, G_m (U-factor technique), and the output noise temperature as a function of the bath temperature. Filled symbols are at 7 mV and 0.23-mA bias point. Open symbols are the maximum output noise temperature and the corresponding mixer conversion gain providing the same receiver noise temperature as at the discussed bias point.

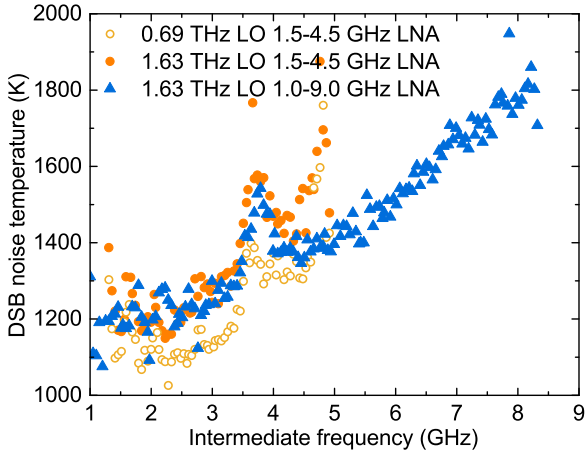

Fig. 9. Receiver noise as a function of the intermediate frequency recorded at 5 K. Filled symbols: 1.63 THz LO. Open symbols: 0.69-THz LO. Circles: 1.5-4.5-GHz LNA. Triangles: 1.0–9.0-GHz LNA.

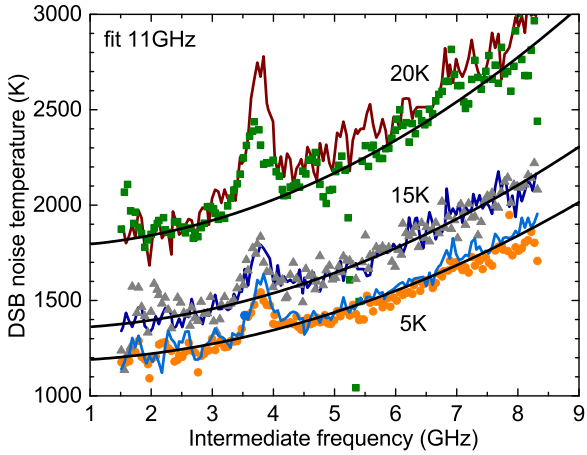

Fig. 10. Receiver noise (at 1.63-THz LO) as a function of the intermediate frequency recorded at 5-, 15-, and 20-K operation temperatures. Results for mixers #10–7 (line), and #10–8 (symbols) are shown.

(see Fig. 8). Apart from a lower LO power, operation at IV3 has an advantage of higher output noise. With an output noise of 220 K (see Fig. 8), the IF LNA noise becomes much less critical to the receiver noise temperature

$$T_r = \frac{1}{2} \cdot L_{\rm opt} \cdot G_m \cdot (T_{\rm out} + T_{\rm if}). \tag{4}$$

This is particularly important for broadband IF LNAs. An LNA optimization can now be focused on input matching rather than on noise, hence eliminating a need for an isolator. In Fig. 8, both the maximum output noise temperature and the corresponding mixer gain (within the minimum T_r zone) are plotted for 5, 15, and 20 K mixer temperatures.

IV-5 (Figs. 4–6) corresponds to the optimal LO power at temperatures from 5 to 20 K. This is the reason why T_r, $P_{\rm LO}$, and relative mixer gain ($S_{\rm mix}$) corresponding to this IV were selected for comparison in Fig. 1. Theoretically, $P_{\rm LO}$ can be estimated from the steady state heat balance equations

$$G \cdot (T_e^n + T_s^n) = P_{\rm LO} + P_{\rm dc} \tag{5}$$

where T_e and T_p are electron and phonon temperatures, respectively, $P_{\rm dc}$ is the Joule heating due to dc bias current, both *G* and *n* are material parameters. *G* corresponds to the total heat conductance from electrons to the heat bath (the substrate, if the electron diffusion is weak, as it is the case in MgB_2 HEB mixers). Coefficient *n* can be estimated [16] from the temperature dependence of the HEB response time and temperature dependences of the heat capacitance. For example, if film-substrate thermal resistance dominates electron cooling process, phonon dynamics will play the major roll. In this case, $n = 4$ [17]. On contrary, for very thin films with a negligible thermal resistance to the substrate, electron–phonon interaction will determine the constant *n*. In NbN HEB mixers, *n* of about 3.6 has been reported by several groups [18], [19]. This value points on a transition for the electron cooling from being phonon-substrate limited to being electron–phonon limited. By fitting our data $P_{\rm LO}(T)$ with (5), we obtain $n = 2 + -0.3$ and $\rm Tc = 29.8 + -1$ K. This value for *n* confirms conclusions made in literature [20] that MgB_2 films have very low thermal resistance towards substrate, and hence, electron–phonon heat transfer to be the limiting factor in the electron cooling for very thin MgB_2 films.

C. Noise Bandwidth

To obtain the HEB receiver NBW, the Y-factor was measured across a wide IF band with an IF step of 50 MHz. Both a 1.5–4.5-GHz and a 1.0–9.0-GHz IF LNA were used for these experiments. Intentions with measurements using the 1.5–4.5-GHz LNA were to verify whether HEB-LNA interference might be affecting the obtained results. In Fig. 9, we show the receiver noise temperature measured with the 1.5–4.5 GHz LNA at both 0.69- and 1.63-THz LOs. The noise temperature increases proportionally over the whole IF range, indicating that NBW is the same at both LOs, and hence, supporting the idea of the bolometric nature of the heterodyne response in discussed devices. The noise temperature curve as measured with the 1.5–4.5-GHz LNA fully overlaps with the data obtained using the 1.0–9.0-GHz LNA at the corresponding IFs. The hump, seen at

3.7-GHz, is present in both data sets, and hence, originates from the bias-T, used for both experiments.

The noise temperature spectrum at 1.63-THz LO was measured at 5, 15, and 20 K for two HEBs from the same batch (see Fig. 10). The fitting curves are for an 11-GHz NBW. Curves for both devices totally overlap, hence indicating good reproducibility of results.

IV. Conclusion

Using both mixing experiments at 0.69 THz and the U-factor technique, we demonstrate that MgB_2 HEB mixers gain variation versus temperature is proportional to LO power. Simultaneously, output mixer noise temperature is nearly constant from 5 up to 20 K. In order to improve mixer gain at 20 K (and, hence, receiver noise temperature), utilization of devices with a higher T_c seems to be a clear direction.

A high value of the output noise ($\sim$200 K) reduces requirements for the IF LNA noise. This property might appear very useful for reduction of the IF ripples, which occur between the HEB and the LNA due to impedance mismatch. For example, for broadband LNAs, input matching (S11) could be > -3 dB. In this case, even a simple 3-dB attenuator would increase the IF chain noise temperature from 5 to 15 K without a noticeable degradation of T_r, but will improve the HEB-LNA matching by 6 dB. In general, the high output noise of MgB_2 HEBs allows us for LNA optimization aiming at a low S11 rather than at a low noise temperature.

Experimental verification of MgB_2 HEB mixers with both the Y-factor and mixing techniques coincide fully, thus dismissing the issue of direct detection effect on the measured Y-factor. Furthermore, mixer sensitivity data for a much broader bias voltage, operation temperatures, and LO power ranges can be obtained compared to the Y-factor technique.

Our preliminary data indicate that MgB_2 HEB mixers can be fabricated with a T_c of 33–34 K (quite feasible with an improved fabrication procedure). In this case, receiver noise temperature at 20 K will greatly improve. This feature is of particular interest for systems where compact mechanical cryocoolers are required (e.g., for space borne instruments).

References

[1] E. Novoselov and S. Cherednichenko, "Low noise terahertz MgB_2 hot-electron bolometer mixers with an 11 GHz bandwidth," *Appl. Phys. Lett.*, vol. 110, no. 3, Jan. 2017, Art. no. 032601.

[2] S. Bevilacqua, E. Novoselov, S. Cherednichenko, S. Shibata, and Y. Tokura, "MgB_2 hot-electron bolometer mixers at terahertz frequencies," *IEEE Trans. Appl. Supercond.*, vol. 25, no. 3, Jun. 2015, Art. no. 2301104.

[3] E. Novoselov, S. Bevilacqua, S. Cherednichenko, S. Shibata, and Y. Tokura, "Effect of the critical and operational temperatures on the sensitivity of MgB_2 HEB mixers," *IEEE Trans. THz Sci. Technol.*, vol. 6, no. 2, pp. 238–244, Mar. 2016.

[4] E. Novoselov, N. Zhang, and S. Cherednichenko, "MgB_2 hot-electron bolometer mixers for THz heterodyne instruments," *Proc. SPIE*, vol. 9914, Jul. 2016, Art. no. 99141N.

[5] E. Novoselov and S. Cherednichenko, "Broadband MgB_2 hot-electron bolometer THz mixers operating up to 20 K," *IEEE Trans. Appl. Supercond.*, vol. 27, no. 4, Jun. 2017, Art. no.

[6] D. Cunnane *et al.*, "Characterization of MgB_2 superconducting hot electron bolometers," *IEEE Trans. Appl. Supercond.*, vol. 25, no. 3, Jun. 2015, Art. no. 2300206.

[7] D. Cunnane *et al.*, "Optimization of parameters of MgB_2 hot-electron bolometers," *IEEE Trans. Appl. Supercond.*, vol. 27, no. 4, Jun. 2017, Art. no. 2300405.

[8] M. A. Wolak *et al.*, "Fabrication and characterization of ultrathin MgB_2 films for hot-electron bolometer applications," *IEEE Trans. Appl. Supercond.*, vol. 25, no. 3, Jun. 2015, Art. no. 7500905.

[9] N. Acharya *et al.*, "MgB_2 ultrathin films fabricated by hybrid physical chemical vapor deposition and ion milling," *APL Mater.*, vol. 4, no. 8, Aug. 2016, Art. no. 086114.

[10] N. Acharya *et al.*, "As-grown versus ion-milled MgB_2 ultrathin films for THz sensor applications," *IEEE Trans. Appl. Supercond.*, vol. 27, no. 4, Jun. 2017, Art. no. 2300304.

[11] E. Novoselov, N. Zhang, and S. Cherednichenko, "Study of MgB_2 ultrathin films in submicron size bridges," *IEEE Trans. Appl. Supercond.*, vol. 27, no. 4, Jun. 2017, Art. no. 7500605.

[12] Virginia Diodes, Inc., Charlottesville, VA, USA. [Online]. Available: http://www.vadiodes.com

[13] S. Cherednichenko, V. Drakinskiy, T. Berg, E. Kollberg, and I. Angelov, "The direct detection effect in the hot-electron bolometer mixer sensitivity calibration," *IEEE Trans. Microw. Theory Techn.*, vol. 55, no. 3, pp. 504–510, Mar. 2007.

[14] H. Ekström, B. Karasik, E. Kollberg, and K. S. Yngvesson, "Conversion gain and noise of niobium superconducting hot-electron mixers," *IEEE Trans. Microw. Theory Techn.*, vol. 43, no. 4, pp. 938–947, Apr. 1995.

[15] F. Arams, C. Allen, B. Peyton, and E. Sard, "Millimeter mixing and detection in bulk InSb," *Proc. IEEE*, vol. 54, no. 4, pp. 612–622, Apr. 1966.

[16] E. M. Gershenzon *et al.*, "Millimeter and submillimeter range mixer based on electronic heating of superconducting films in the resistive state," *Sov. Phys. Supercond.*, vol. 3, no. 10, p. 1582, 1990.

[17] W. A. Little, "The transport of heat between dissimilar solids at low temperatures," *Can. J. Phys.*, vol. 37, pp. 334–349, 1959.

[18] S. Cherednichenko *et al.*, "Local oscillator power requirement and saturation effects in NbN HEB mixers," in *Proc. 12th Int. Symp. Space THz Technol.*, 2001, pp. 273–285.

[19] W. Zhang *et al.*, "Temperature dependence of the receiver noise temperature and IF bandwidth of superconducting hot electron bolometer mixers," *Supercond. Sci. Technol.*, vol. 27, 2014, Art. no. 085013.

[20] S. Cherednichenko, V. Drakinskiy, K. Ueda, and T. Naito, *Appl. Phys.Lett.*, vol. 90, no. 2, Jan. 2007, Art. no. 023507.

Evgenii Novoselov was born in Saint-Petersburg, Russia, in 1988. He received the B.Sc. degree and M.Sc. degree (*summa cum laude*) from the Saint-Petersburg National Research University of Information Technologies, Mechanics and Optics (NRU ITMO), Saint-Petersburg, in 2009 and 2011, respectively. He is currently working toward the Ph.D. degree at the Terahertz Millimetre Wave Laboratory, Chalmers University of Technology, Göteborg, Sweden, working on MgB_2 hot electron bolometers.

During his studies with the university, he worked with the research center "Femtosecond Optics and Femtotechnology," NRU ITMO, during 2007–2011. There he participated in a number of projects on the development of terahertz spectrography and reflectometry using TDS. After completing the Master's degree, he joined LLC "TELROS Integration," Saint-Petersburg, as a Communication Systems Design Engineer during 2011–2013.

Sergey Cherednichenko was born in Mariupol, Ukraine, in 1970. He received the Diploma degree (Hons.) in physics from the Taganrog State Pedagogical Institute, Taganrog, Russia, in 1993, and the Ph.D. degree in physics from Moscow State Pedagogical University, Moscow, Russia, in 1999.

From 2000 to 2006, he was involved in the development of terahertz band superconducting mixers with the Herschel Space Observatory; and from 2008 to 2009, in the water vapour radiometer for ALMA. Since 2007, he has been an Associate Professor with the Department of Microtechnology and Nanoscience, Chalmers University of Technology, Gothenburg, Sweden. His research interests include terahertz heterodyne receivers and mixers, photon detectors, THz antennas and optics, thin superconducting films and their application for THz and photonics, and material properties at THz frequencies.